Chalcogenide Letters Vol. 22, No. 7, July 2025, p. 637 - 648

Modeling and optimization of a CZT(S,Se)-based tandem solar cell

B. Yassine, B. Tahar *, G. Fathi, B. Meriem, B. Ibtissem
LNCSM, Department of Physics, ENS Kouba, Alger, Algeria

In this paper, we designed a two-junction (tandem) solar cell model (tandem solar cell), consisting of an top and bottom subcell with absorber layers of Cu_2SnZnS_4 (CZTS) and $Cu_2SnZnSe_4$ (CZTSe) materials, respectively, for each subcell with a ZnS buffer layer and a ZnO window layer. This model was validated using the SCAPS-1D numerical simulation program. We also optimized the performance of the tandem cell as a whole using the simulation by studying the effect of the thickness of the absorber layer of the top subcell and the thickness of the absorber layer of the bottom subcell and its doping. The results of the study gave the optimal thickness value X_{CZTS}=142,8nm for the top subcell absorber layer, the optimal thickness value X_{CZTSe}=1µm for the bootom subcell absorber layer and its optimal doping value $N_{A/CZTSe}=10^{19}cm^{-3}$ Tandem cell characteristics corresponding to these optimal values are open-circuit voltage V_{oc}=1,4861V, short circuit current J_{sc}=18,59mA/cm^2, fill factor FF=73.12% and efficiency ηˌ=20,20%.

(Received January 30, 2025; Accepted July 16, 2025)

Keywords: Solar cell, Thickness, Doping, Tandem, Absorber layer, Efficiency

1. Introduction

Thin-film solar cells have received significant attention over the past few decades due to the increased demand for electricity and the substantial scientific advancements that have facilitated their production. Among the thin-film cells that researchers have focused on developing are CdTe cells, $CuInS_2$ (CIS) cells, and $CuInGaSe_2$ (CIGS) cells. However, there are several limitations that constrain their production and use in energy generation, including the scarcity and high cost of materials like In, Ga, and Te, and the hazards posed by some toxic materials, such as cadmium (Cd). Therefore, there is a need to find materials composed of more abundant and less toxic elements [1].

The solar cells made from the semiconductor $Cu_2SnZn(S,Se)_4$ (CZTSSe) are considered excellent, low-cost alternatives because all the chemical elements in this compound are abundant, environmentally friendly, and non-toxic [1]. CZTSSe materials have good physical properties, including a high absorption coefficient exceeding 10^4cm^{-1} and a direct band gap (E_g) that can be tuned between 1eV and 1,5eV depending on the Se content in the semiconductor. Additionally, even the classic CdS buffer layer in this type of cell can be replaced with a ZnS layer according to various sources. The experimental efficiency of single-junction CZTSSe solar cells has reached 12,6%, as reported in the literature [2,3].

Significant efforts are currently being made to improve the performance of this type of cell and increase its efficiency. Among the methods and techniques that could help achieve this are the fabrication of tandem CZTSSe solar cells, which are cells with two pn junctions. A tandem cell consists of two sub-cells (one placed on top of the other), each with a different energy bandgap, so that the top cell has a larger bandgap compared to the bottom cell. This design allows each cell to be more effective at absorbing photons of specific wavelengths [5,6].

In this research, a model for a tandem CZTSSe solar cell structure was designed and its feasibility was verified using the SCAPS-1D simulation program. The performance of the tandem cell structure was then optimized by studying the effect of the absorber layer thickness in both the top and bottom cells, as well as the impact of doping the absorber layer of the bottom cell.

* Corresponding author: tahar.belal@g.ens-kouba.dz
https://doi.org/10.15251/CL.2025.227.637

2. Materials and methods

2.1. Tandem solar cell structure

Based on reference [6], we propose a tandem soller cell model consisting of two thin-layer sub-cells. The window layer of both cells is ZnO, the buffer layer is ZnS, the absorber layer of the top cell is Cu_2SnZnS_4 (CZTS) and the absorber layer of the bottom cell is $Cu_2SnZnSe_4$ (CZTSe). The CZTS absorber layer has a larger E_g energy gap compared to CZTSe. The two sub-cells are electrically connected in series and placed on the same optical path so that photons not absorbed by the top cell penetrate and reach the bottom cell (Figure 1).

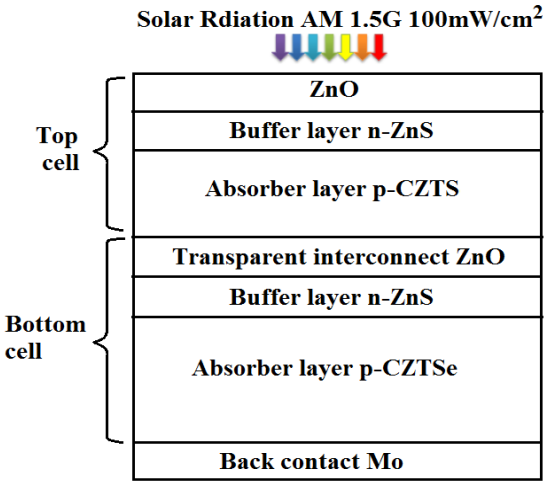

Fig. 1. Tandem cell structure.

2.2. Simulation parameters

The parameters of the different cell layers are listed in Table 1.

Table 1. Tandem cell parameters.

Parameter	CZTS [4,7,11]	CZTSe [3,8,9,10]	ZnS [3,11]	ZnO [3,11]
Band gap E_g(ev)	1.5	1	3.7	3.37
Electron affinity (eV)	4.5	4.1	4.5	4.4
Dielectric permittivity	10	13.6	9	9
CB effective density of states (cm^{-3})	$2{,}2 \times 10^{18}$	$2{,}2 \times 10^{18}$	$2{,}2 \times 10^{18}$	$2{,}2 \times 10^{18}$
VB effective density of states (cm^{-3})	$1{,}8 \times 10^{19}$	$1{,}8 \times 10^{19}$	$1{,}8 \times 10^{19}$	$1{,}8 \times 10^{19}$
Electron thermal velocity (cm/s)	10^7	10^7	10^7	10^7
Hole thermal velocity (cm/s)	10^7	10^7	10^7	10^7
Electron mobility (cm^2/V.s)	100	100	100	100
Hole mobility (cm^2/V.s)	25	25	25	25
Shallow uniform acceptor density, NA (cm^{-3})	10^{17}	10^{17}	0	0
Shallow uniform donor density, ND (cm^{-3})	10	10	10^{18}	10^{17}
Thickness X(µm)	0,5	0,5	0,05	0,05
contact properties	Front contact [7]		Back contact [7]	
Surface recombination velocity of electron S_e(cm/s)	10^7		10^7	
Surface recombination velocity of hole S_h(cm/s)	10^7		10^7	

Temperature T=300K, parallel resistance is infinite and series resistance is zero. the incoming solar spectrum as $AM_{1.5}$ and its power as P_{in} =100mW/cm^2.

3. Results and discussion

First, we simulate the two sub-cells individually with the incoming solar spectrum as $AM_{1.5}$ and its power as P_{in}=100mW/cm^2 to verify the applicability of the proposed model. The simulation results are listed in Table 2.

Table 2. Characteristics of the two subcells under $AM_{1.5}$ solar spectrum.

	V_{co}(v)	J_{sc} (mA/cm^2)	FF(%)	η(%)
CZTS cell	0,9511	25,9021	65,72	16,19
CZTSe cell	0,4891	38,5767	66,27	12,50

The characteristics of the tandem cell as a whole cannot be obtained using the SCAPS simulation program but can be calculated by simulating the top subcell as the solar spectrum reaching it is $AM_{1.5}$ and the bottom subcell as only the portion of the solar spectrum passing through the top cell or not absorbed by the top cell.

If $J_{sc.top}$ is the short-circuit current density of the top subcell and $J_{sc.bot}$ is the short-circuit current density of the bottom subcell, then the tandem cell's short-circuit current density $J_{sc.tan}$ is [12,13]:

$$J_{sc.tan} = \min (J_{sc.top} \text{ et } J_{sc.bot}) \quad (1)$$

In the case of $J_{sc.top} = J_{sc.bot}$ then [12,14]:

$$J_{sc.tan} = J_{sc.top} = J_{sc.bot} \quad (2)$$

If $V_{co.top}$ is the open circuit voltage of the top sub-cell and $V_{co.bot}$ is the open circuit voltage of the bottom sub-cell then the open circuit voltage of the tandem cell $V_{co.tan}$ is [14,15]:

$$V_{oc.tan} = V_{oc.top} + V_{oc.bot} \quad (3)$$

The maximum power P_m and the fill factor FF of the tandem cell are given by [16]:

$$P_m = V_m . I_m \quad (4)$$

$$FF_{tan} = \frac{V_m . I_m}{V_{co.tan} . I_{sc.tan}} \quad (5)$$

where I_m and V_m are the current and voltage corresponding to the maximum power.

The efficiency η_{tan} of a tandem cell is given by:

$$\eta_{tan} = \frac{V_{oc.tan} . I_{sc.tan}}{P} FF_{tan} \quad (6)$$

The J-V characteristic of the subcells and tandem cell is represented in Figure 2.

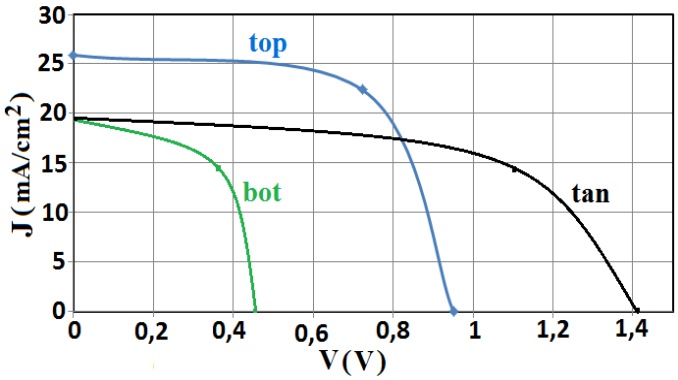

Fig. 2. J-V characteristic of the subcells and tandem cell.

The other characteristics of the two subcells and the tandem cell are listed in Table 3.

Table 3. Characteristics of the two subcells under AM1.5 solar spectrum.

	V_{oc}(v)	J_{sc} (mA/cm^2)	FF(%)	η(%)
CZTS cell	0,9511	25,9021	65,72	16,19
CZTSe cell	0,4661	18,5161	62,32	10,22
Tandem cell	1,4172	18,5161	59,82	15,70

The efficiency of the tandem cell is limited to 15,70% due to the loss of current due to the large difference in the current density $J_{sc,top}$ (25,9021mA/cm^2) generated by the top subcell and $J_{sc,bot}$ (18,5161mA/cm^2) generated by the botom subcell. This large difference in the value of the Jsc current density is due to the fact that only a small percentage of photons reach the bottom subcell because most of them have been absorbed at the level of the top subcell.

In order for the tandem cell efficiency to be maximized, the current densities $J_{sc.top}$ and $J_{sc.bot}$ generated by the top and bottom subcells must be equal (matching current condition), in this case the current density $J_{sc.tan}$ generated by the whole tandem cell structure (also denoted as $J_{sc.matched}$) is equal to $J_{sc.top}$ and $J_{sc.bot}$ [6,17].

$$J_{sc.matched} = J_{sc.top} = J_{sc.bot} \quad (7)$$

To improve the efficiency of the previously obtained tandem cell, we modify its parameters, namely the thickness X_{CZTS} of the absorbent layer CZTS of the top subcell and the thickness X_{CZTSe} of the bottom subcell, and doping it with $N_{A/CZTSe}$. We search for their optimal values that satisfy the condition that $J_{sc.top}$ and $J_{sc.bot}$ are equal.

3.1. Effect of X_{CZTS} thickness

We study the effect of the thickness of the absorbent layer of the top subcell X_{CZTS} on the properties of the top and bottom subcells and the tandem cell as a whole by simulation, changing its value from 0,1µm to 0,5µm. The changes in the properties of the two subcells and the tandem cell in terms of the X_{CZTS} fish are represented in the following figure.

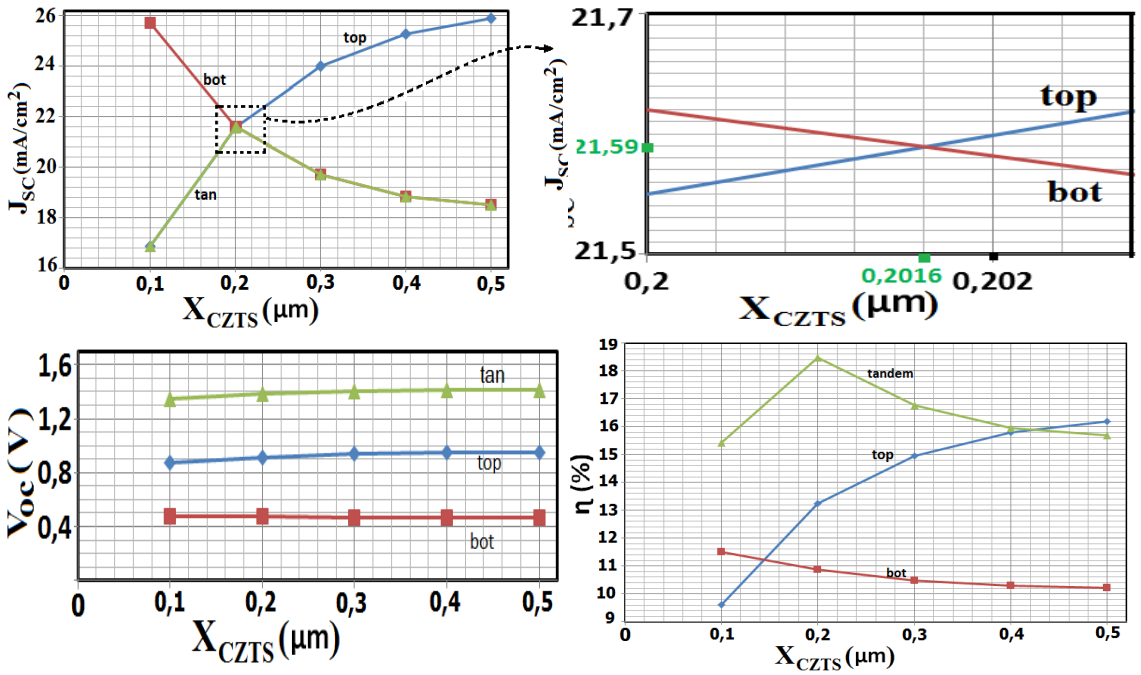

Fig. 3. Characteristic changes of the two sub-cells and the tandem cell in terms of the X_{CZTS} thickness.

For the top cell, when X_{CZTS} was increased from 0,1µm to 0,5µm, the open-circuit voltage $V_{co.top}$ and the current density $J_{sc.top}$ also increased, and as a result, the efficiency η_{top} also increased from 9,92% to 16,19%. The explanation for these observations is that low-energy photons (photons with large wavelengths) are absorbed by the absorber layer when the latter is thicker. Increasing the number of absorbed photons increases the number of electron-hole pairs that are generated in the CZTS absorber layer, and as a result, the $J_{sc.top}$ current density increases and the η_{top} efficiency increases [18,17,7]. For a small thickness, the phenomenon of electron-hole pair generation occurs near the interfaces of the absorber layer where the high density of defects that are recombination centers for the generated electron-hole pairs, so their presence reduces the number of electrons and holes collected and the current density $J_{sc.top}$ decreases and the efficiency η_{top} decreases as a result. The larger the thickness, the farther the electron-hole pair generation phenomenon is from the surface of the absorber layer and the greater the efficiency.

For the bottom sub-cell, increasing the thickness X_{CZTS} did not significantly affect the open circuit voltage $V_{oc.bot}$ but caused a significant decrease in the current density $J_{sc.bot}$, which also led to a decrease in the efficiency η_{bot}. The explanation for these results is that a large part of the solar spectrum that could have been absorbed by the bottom subcell was absorbed at the level of the top subcell, and the thicker the X_{CZTS}, the more light absorption at the level of the upper subcell, the fewer photons reach the front surface of the lower subcell, and the bottom the current density of the $J_{sc.bot}$ generated by its efficiency η_{bot} as a result [6,17].

For a tandem cell, its characteristics are mainly related to the characteristics of the two subcells as explained above. The open-circuit voltage $V_{oc.tan}$ is not much affected by changing the thickness X_{CZTS}, while the compartment current density $J_{sc.tan}$, which is the lowest of the two currents $J_{sc.top}$ and $J_{sc.bot}$ generated by the two subcells, and its output η_{tan} change in a non-monotonic manner as:

-When the X_{CZTS} thickness increases from 0,1µm to 0,2016µm, the current density $J_{sc.tan}$ increases from 16,37mA/cm^2 to 21,59 mA/cm^2 ($J_{sc.tan}$ is equal to $J_{sc.top}$ which is the smallest current in this field) and ηtan increases from a value of 15,42% to reach its maximum value of 19,69%.

-When increasing the X_{CZTS} thickness value from 0,2016µm to 0,5µm, the current density $J_{sc.tan}$ decreases from its maximum value of 21,59mA/cm^2 to 18,51mA/cm^2 ($J_{sc.tan}$ is equal to $J_{sc.bot}$ which is the smallest current in this field) and the efficiency η_{tan} also decreases from 19,69% to 18,51%.

From these results, the optimal thickness value that allows the condition of $J_{sc.top}$ and $J_{sc.bot}$ being equal (the value corresponding to $J_{sc.matched}$) and makes the two sub-cells work harmoniously is X_{CZTS}=201,6nm. At this value, the η_{tan} tandem cell achieves the highest efficiency (19,69%). The characteristics of the tandem cell and the two subcells are listed in Table 4.

Table 4. Characteristics of the tandem cell and the two subcells after X_{CZTS} thickness optimization.

	V_{oc}(v)	J_{sc} (mA/cm^2)	FF(%)	η(%)
Top cell (x_{CZTS}=201,6nm)	0,9165	21,59	67,18	13,30
bottom cell (x_{CZTSe}=500nm)	0,4704	21,59	63,21	10,80
tandem cell	1,3869	21,59	65,82	19,70

In the next step, we optimize the performance of the tandem cell and increase its efficiency by modifying the X_{CZTSe} thickness and $N_{A/CZTSe}$ doping of the absorbent layer of the bottom sub-cell, always keeping in mind that the performance of the bottom sub-cell is also affected by the X_{CZTS} thickness, which controls and determines the part of the solar spectrum that reaches it, so we attach great importance to the X_{CZTS} value when simulating the bottom cell.

3.2. Effect of X_{CZTSe} thickness

We study the effect of the thickness X_{CZTSe} of the absorber layer CZTSe of the bottom subcell on its performance and on the performance of the tandem cell as a whole. Figure 4 represents the $J_{sc.top}(X_{CZTS})$ curve of the current produced by the top cell (the same curve we obtained when studying the effect of X_{CZTS} thickness) and the $J_{sc.bot}(X_{CZTS})$ curves corresponding to X_{CZTSe} thickness values between 0,5µm and 3µm.

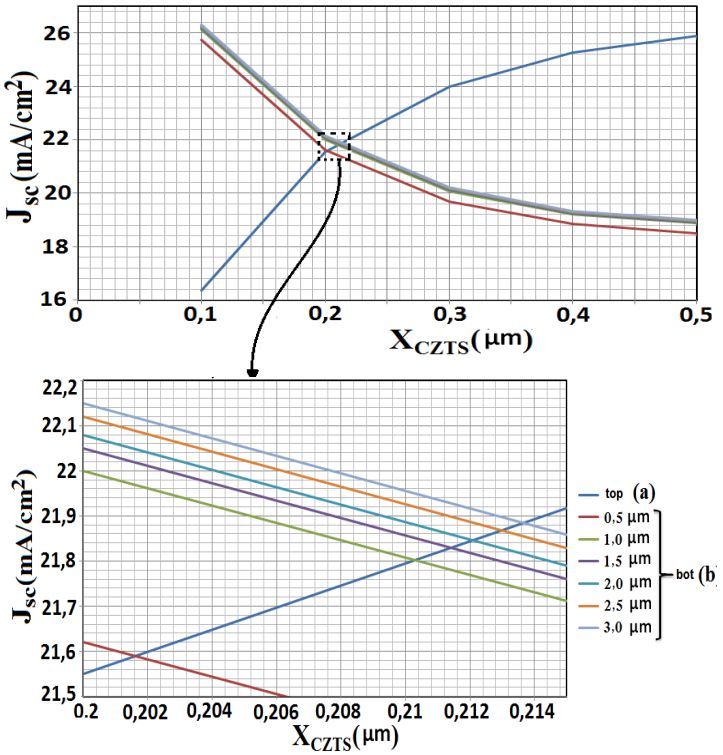

Fig. 4. (a) Changes of $J_{sc.top}$ in terms of X_{CZTS} thickness; (b) Changes of $J_{sc.bot}$ in terms of X_{CZTS} thickness for different X_{CZTSe} thickness values.

Figure 5 and Table 5 represent the X_{CZTSe} and X_{CZTS} thickness values for which $J_{sc.bot}$ and $J_{sc.top}$ are equal (X_{CZTSe} and X_{CZTS} thickness values corresponding to $J_{sc.matched}$), for which the top and bottom sub-cells work in harmony and the tandem cell has the highest possible conversion efficiency. The values of X_{CZTSe} and X_{CZTS} are determined by the intersection points of the $J_{sc.top}(X_{CZTS})$ and $J_{sc.bot}(X_{CZTS})$ curves shown in Figure 4.

Table 5. Thickness X_{CZTS} and thickness X_{CZTSe} values corresponding to $J_{sc.top}$ and $J_{sc.bot}$ isochrones.

X_{CZTSe} (µm)	0,5	1	1,5	2	2,5	3
X_{CZTS} (nm)	201,6	210,3	211,4	212,1	213,0	213,7

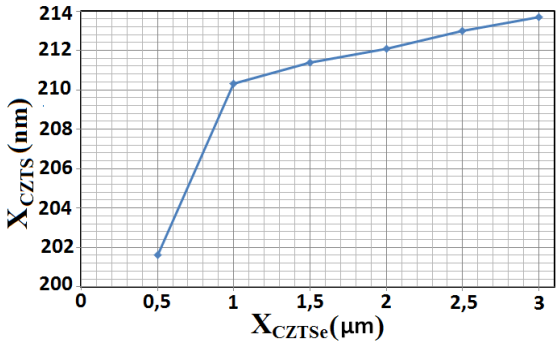

Fig. 5. Thickness X_{CZTS} and thickness X_{CZTSe} values corresponding to $J_{sc.top}$ and $J_{sc.bot}$ equality.

The two subcells generate equal $J_{sc.bot}$ and $J_{sc.top}$ currents when X_{CZTSe} is 0,5µm thick and X_{CZTS} is 201,6nm thick. When X_{CZTSe} is increased to 3µm, X_{CZTS} must be increased to 213,7nm. In general, when X_{CZTSe} is increased by a certain amount, X_{CZTS} must also be increased by a certain amount so that the two subcells generate equal $J_{sc.bot}$ and $J_{sc.top}$ currents and so that the tandem cell has the highest efficiency. Figure 6 shows the changes of the tandem cell characteristics in terms of the thickness X_{CZTSe}.

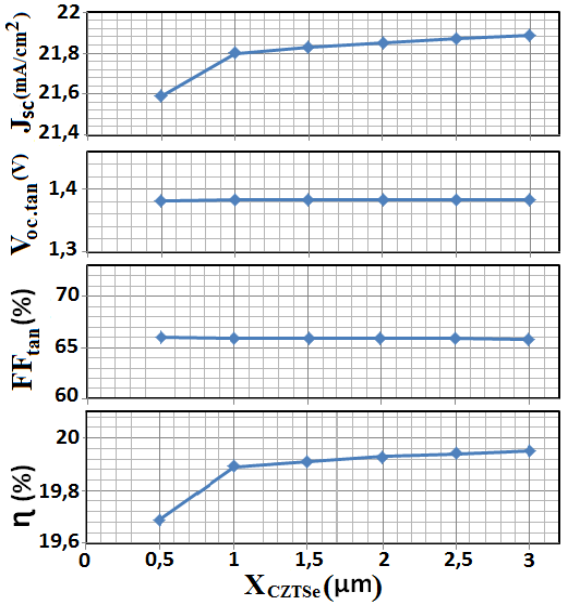

Fig. 6. Tandem cell property changes in relation to the X_{CZTSe} thickness.

Increasing the X_{CZTSe} thickness from 0,5µm to 1µm (corresponding to increasing the X_{CZTSe} thickness from 201,6nm to 210,3nm) did not significantly affect the open circuit voltage $V_{oc.tan}$ but increased the current density $J_{sc.tan}$ generated by the tandem cell from 21,59mA/cm^2 to 21,80mA/cm^2. The explanation for this result is that increasing X_{CZTSe} (and increasing X_{CZTSe} as well, which is imposed by the J_{sc} Matched condition) leads to an increase in photon absorption at the cell level and thus increases the generation of electron-hole pairs, increasing the current density $J_{sc.tan}$ ($J_{sc.matched}$) generated by the tandem cell structure and, as a result, its yield value increased from 19,69% to 19,89%.

The significant increase in X_{CZTSe} thickness from 1µm to 3µm (corresponding to the increase in X_{CZTS} thickness from 201,6nm to 213,7nm) also did not affect the open circuit voltage $V_{oc.tan}$, while the current density $J_{sc.tan}$ increased slightly from 21,80mA/cm^2 to 21,89mA/cm^2, which increased the efficiency value η_{tan} from 19,89% to 19,95% only because the limited X_{CZTSe}=1µm thickness (corresponding to X_{CZTS}=210,4nm) is sufficient to absorb most of the photons reaching the tandem cell structure. It is economically pointless to increase the thickness of X_{CZTSe} (more raw material for cell fabrication) for very little increase in yield η_{tan} [18], so we consider 1µm X_{CZTSe} to be an optimal value. The sub-cell and tandem cell characteristics for this value are listed in Table 6.

Table 6. Characteristics of the tandem cell and the two sub-cells after thickness optimization X_{CZTSe}.

	$J_{sc.matched}$(mA/cm^2)	V_{oc}(v)	FF(%)	η(%)
Top cell (x_{CZTSe}=1µm)	21,80	0,9120	67,47	13,415
Bottom cell (x_{CZTS}=201,6nm)	21,80	0,4713	63,13	11,03
Tandem cell	21,80	1,3833	65,95	19,89

3.3. Effect of doping $N_{A/CZTSe}$

We study the effect of $N_{A/CZTSe}$ doping of the CZTSe absorber layer of the bottom subcell on its performance and on the performance of the tandem cell as a whole. Figure 7 represents the $J_{sc.top}(X_{CZTS})$ curve of the current produced by the top cell (the same curve we obtained when studying the effect of X_{CZTS} thickness) and the $J_{sc.bot}(X_{CZTS})$ curves corresponding to $N_{A/CZTSe}$ doping values between 10^{15}cm^{-3} and 10^{20}cm^{-3}.

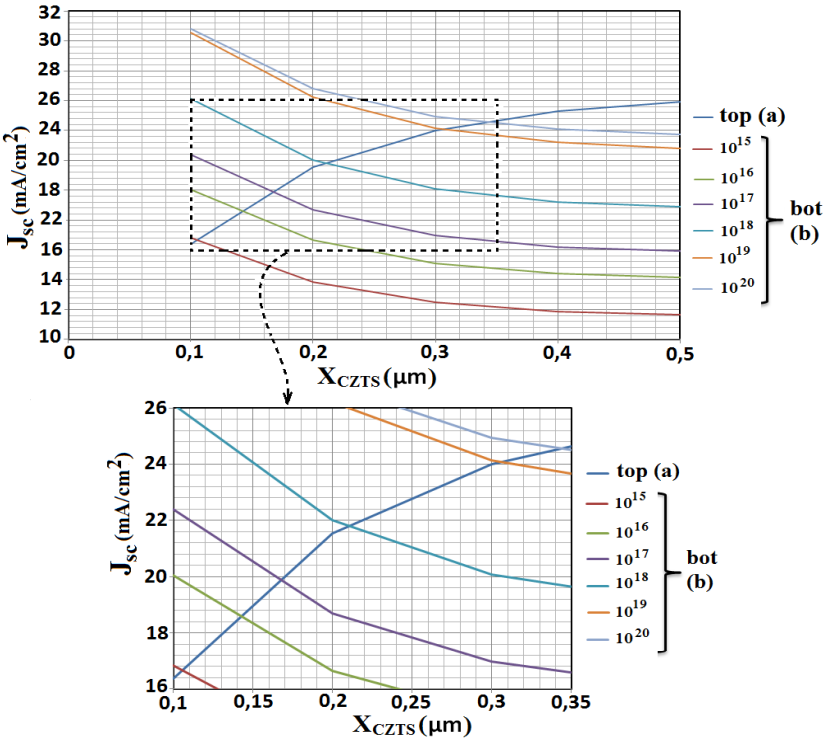

Fig. 7. (a) $J_{sc.top}$ changes in terms of X_{CZTS} thickness; (b) $J_{sc.bot}$ changes in terms of X_{CZTS} thickness for different $N_{A/CZTSe}$ doping values.

Figure 8 and Table 7 represent the $N_{A/CZTSe}$ and X_{CZTS} values for which the $J_{sc.bot}$ and $J_{sc.top}$ currents are equal, for which the top and bottom subcells are harmonized, and for which the tandem cell has the greatest possible conversion yield. The values of $N_{A/CZTSe}$ and X_{CZTS} are determined by the intersection points of the $J_{sc.top}(X_{CZTS})$ and $J_{sc.bot}(X_{CZTS})$ curves.

Table 7. $N_{A/CZTSe}$ and X_{CZTSe} doping values corresponding to $J_{sc.top}$ and $J_{sc.bot}$. isochrones.

$N_{A/CZTSe}$ (cm^{-3})	10^{15}	10^{16}	10^{17}	10^{18}	10^{19}	10^{20}
X_{CZTS} (nm)	343,7	306,3	210,3	167,8	142,8	106,6

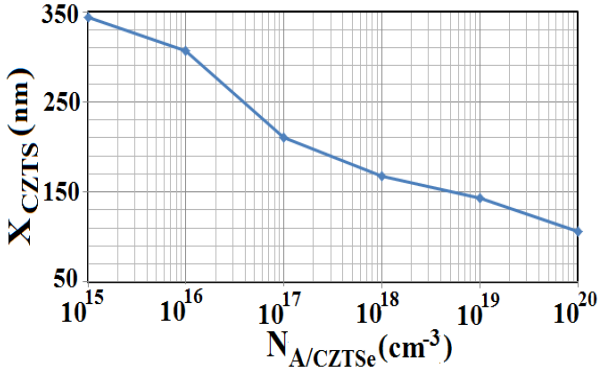

Fig. 8. $N_{A/CZTSe}$ doping and X_{CZTS} thickness corresponding to the equality of $J_{sc.top}$ and $J_{sc.bot}$.

The two subcells generate equal $J_{sc.bot}$ and $J_{sc.top}$ currents when $N_{A/CZTSe}$ is equal to $10^{15}cm^{-3}$ and X_{CZTS} is equal to 0,340µm. When $N_{A/CZTSe}$ is increased from $10^{15}cm^{-3}$ to $10^{19}cm^{-3}$, X_{CZTS} must be reduced from 0,340µm to 0,142µm. According to these results, when $N_{A/CZTSe}$ is increased by a certain amount, X_{CZTS} should be decreased by a certain amount so that the two sub-cells generate equal $J_{sc.bot}$ and $J_{sc.top}$ currents and the tandem cell has the highest efficiency, as each $N_{A/CZTSe}$ value corresponds to a specific X_{CZTS} value. Figure 9 represents the changes in tandem cell characteristics when $N_{A/CZTSe}$ changes from a value of $10^{15}cm^{-3}$ to a value of $10^{20}cm^{-3}$.

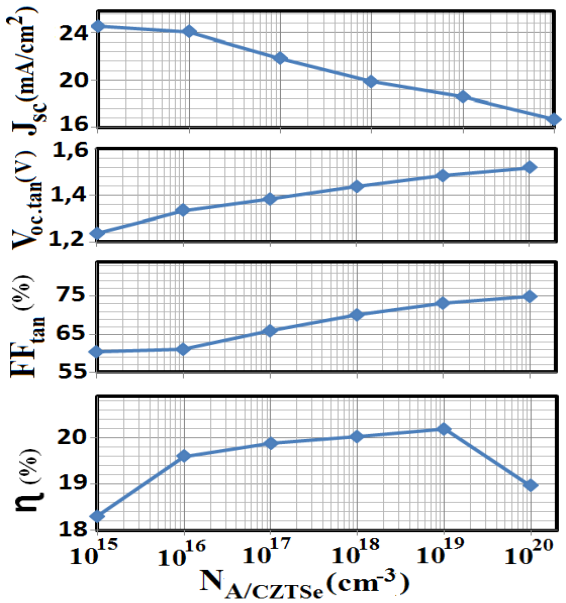

Fig. 9. Tandem cell characteristic changes in relation to $N_{A/CZTSe}$ doping.

According to Figure 9, increasing $N_{A/CZTSe}$ from $10^{15}cm^{-3}$ to $10^{20}cm^{-3}$ (and decreasing X_{CZTS} from 0,340µm to 0,142µm imposed by by the J_{sc} Matched condition) Although it reduced the current density $J_{sc.tan}$ from 24,56mA/cm^2 to 16,66mA/cm^2, it increased the open circuit voltage $V_{co.tan}$ from 1,2350V to 1,5198V and increased the fill factor FF_{tan} from 60,36% to 74,92%, which increased the tandem cell yield ηtan from 18,31% to 20,20%.

The benefit of increasing the doping or defects in semiconductors is to increase the electrical conductivity, but it often exceeds a certain limit and becomes a loss factor, because it causes the recombination phenomenon of electron-hole pairs, the collection of free electrons generated by photoabsorption in the absorber layer decreases more and more, the current density decreases more and more, and the conversion efficiency decreases [7,18,19], so we observed the degradation of the bottom subcell efficiency and the tandem cell efficiency if the $N_{A/CZTSe}$ doping exceeds the value of $10^{19}cm^{-3}$, so we consider this value as an optimal value. The subcell and tandem cell characteristics for this value are listed in Table 8.

Table 8. Characteristics of the tandem cell and the two subcells after X_{CZTSe} thickness optimization.

	$J_{sc.matched}$ (mA/cm^2)	V_{oc}(v)	FF(%)	η(%)
top cell (x_{CZTS}=142,8nm)	18,59	0,8909	68,43	11,32
Bottom cell ($N_{A/CZTSe}=10^{19}cm^{-3}$, x_{CZTSe}=1µm)	18,59	0,5952	80,27	13,75
Tandem cell	18,59	1,4861	73,12	20,20

The voltage-current characteristic of the tandem cell and subcells is represented in Figure 10.

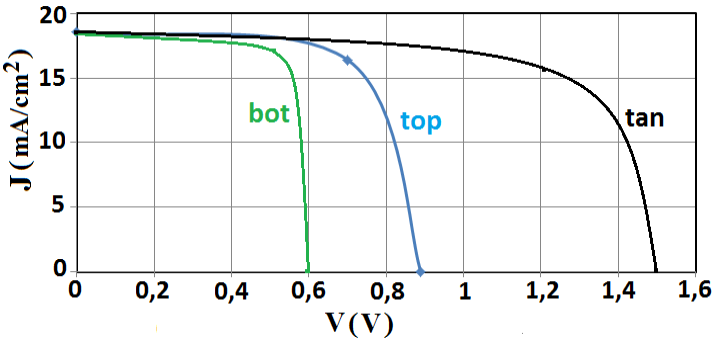

Fig. 10. J-V characteristic of the tandem cell and subcells after optimization.

4. Comparison of tandem cell characteristics before and after optimization

Modifying the parameters of the two sub-cells improved the performance of the tandem cell and thus increased its efficiency from 15,70% to 20,20% as shown in Table 9.

Table 9. Tandem cell properties before and after optimization.

	V_{oc}(v)	J_{sc} (mA/cm^2)	FF(%)	η(%)
Before optimization	1,4172	18,5161	59,82	15,70
after optimization	1,4861	18,6	73,12	20,20

5. Conclusion

In this study, we designed a tandem cell consisting of two subcells, the absorber layer of the top subcell is CZTS and the absorber layer of the bottom subcell is CZTSe, and the buffer layer of each is ZnS. We simulated this cell under $AM_{1.5}$ solar spectrum using SCAPS software. The initially obtained efficiency of the tandem cell was only 15,70% due to the large difference in the values of the current density produced by the top subcell (25,90mA/cm^2) and the bottom subcell (18,51mA/cm^2). Then we studied the effect of the thickness of the CZTS layer as well as the thickness and doping of the CZTSe layer with the aim of searching for their optimal values that increase the ability of the two sub-cells to convert light into electricity and make the performance of the two sub-cells consistent and achieve the matching current condition produced by each cell. The result was an increase in the efficiency to 20,20% and the matching current was 18,59mA/cm^2, while the open circuit voltage was 1,48V and the fill factor was 73,12% for the thickness values X_{CZTS}=142,8nm and X_{CZTSe}=1µm and the doping value $N_{A/CZTSe}$=10^{19}cm^{-3}.

Acknowledgments

The authors gratefully acknowledge to Dr. Marc Burgelman, University of Gent, Belgium, for providing the SCAPS simulation software.

References

[1] Suryawanshi M P, Agawane G L, Bhosale S m, et al., Materials Technology. 2017; 28(1): 98-109; https://doi.org/10.1179/1753555712Y.0000000038

[2] Benmir A, Aida M, Annales des Sciences et Technologie. 2014; 6(1):12- 23; https://doi.org/10.12816/0040256

[3] Chadel M, Chadel A, Bouzaki M, et al., Materials Research Express. 2013; 4(11): 115503; https://doi.org/10.1088/2053-1591/aa95df

[4] Bara Y, Belal T, Ghezal F., Chalcogenide Letters. 2022; 19(8): 503-511; https://doi.org/10.15251/CL.2022.198.503

[5] Baseerat B, Bita F, Waseem R, et al., Journal of Computational Electronics. 2021; 20: 1769-1778; https://doi.org/10.1007/s10825-021-01733-4

[6] Bouanani B, Joti A, Bachir Bouiadjra F, et al., Optik - International Journal for Light and Electron Optics. 2020; 204: 164217; https://doi.org/10.1016/j.ijleo.2020.164217

[7] Mahbub R, Saidul I, Farhana A, et al. South Asian Journal of Engineering and Technology. 2016; 2(52): 1-10.

[8] Kerour S., Cellules solaires en couches minces à base du Cu2SnZn(S,Se)4 et des matériaux non polluants: Etude et optimisation. University of Setif, Algeria, 2022.

[9] Mir Kazem O, Mehran M, Nafiseh M, et al., Solid-State Electronics. 2018; 141: 50-57; https://doi.org/10.1016/j.sse.2017.12.004

[10] Moustafa M, Al Zoubi T, Yasin Set, al., Optik - International Journal for Light and Electron Optics. 221; 247: 167885; https://doi.org/10.1016/j.ijleo.2021.167885

[11] Olawale E O, Adekoya A A, Alabi A B., Moroccan Journal of Chemistry. 2020; 8(3): 673-683.

[12] Elbar M, Etude par simulation numérique d'une cellule solaire en CIGS à multi-jonction par le logiciel Tcad Silvaco, Université Mohamed Khider -Biskra, Algeria, 2018.

[13] Chloe D., Elaboration de films de perovskites hybrides par coévaporation pour des applications photovoltaïques, Université Paris Saclay, 2019.

[14] Jae Hyun P, Su Geun i, Ik Jae P., Exploration .2023; 3(2):20220029; https://doi.org/10.1002/EXP.20220029

[15] Hadipour A. de Boer B, Blom P W M., Organic Electronics, 2008; 9(5): 617-624; https://doi.org/10.1016/j.orgel.2008.03.009

[16] Alireza S, Mohsen H, Farzin S, Optik - International Journal for Light and Electron Optics. 2020; 222: 165461; https://doi.org/10.1016/j.ijleo.2020.165461

[17] Elbar M, Tobbeche S, Merazga A., Solar Energy 2015; 122: 104-112; https://doi.org/10.1016/j.solener.2015.08.029

[18] Joël Hervé N T, Bouchaib H, Jean-Marie N, Afrique SCIENCE .2015; 11(4): 16-23.

[19] Chadel A, Benyoucef B, Chadel M., Optoelectron. Adv. Mat. **5**(9), 653 (2015).